

Dynamical mean-field approximation for unitary Fermi gas

Nir Barnea*

The Racah Institute of Physics, The Hebrew University, 91904 Jerusalem, Israel.

Institute for Nuclear Theory, University of Washington, 98195 Seattle, Washington, USA

(Dated: September 2, 2021)

Dynamical mean-field approximation with explicit pairing is utilized to study the properties of a two-component Fermi gas at unitarity. The problem is approximated by the lattice Hubbard Hamiltonian, and the continuum limit is realized by diluting the lattice. We have found that at zero temperature the predictions of this theory for the energy and the pairing gap agree remarkably well with the results of full numerical Monte-Carlo simulations. Investigating the evolution of the system with temperature we identify the existence of a second order phase transition associated with a jump in the heat capacity and the collapse of the pairing gap.

PACS numbers: 67.85.Lm, 05.30.Fk, 03.75.Ss

Introduction – The properties of a dilute Fermi gas with interparticle distance much larger than the effective range r_e depend on only two parameters. The scattering length, a_s which is sufficient to characterize the interaction and interparticle distance or the Fermi momentum k_F . When the pair interaction is fine tuned to create a two-body bound state with zero energy, the scattering length diverges and the Fermi momentum remains the only length scale. At this point, commonly referred to as unitarity, the system acquires universality, as its properties become independent of the nature of its constituents. Dilute neutron gas where a_s is an order of magnitude larger than r_e is a natural example for such system. Unitarity conditions can also be achieved with cold Fermi atoms fine tuned near a Feshbach resonance [1].

Regardless of the strength of the interaction, the zero temperature ground state of a Fermi gas with attractive two-body force is a superconductor. As the attraction increases the nature of the system changes from a BCS superconductor at weak coupling to a gas of fermionic pairs forming a Bose-Einstein condensation (BEC) at strong coupling. At unitarity the system is in between these two limits and is neither a BCS superconductor nor a BEC.

In this work we apply the dynamic mean field theory (DMFT), introduced over a decade ago by Georges and Kotliar [2], to study the properties of unitary Fermi gas. In this theory, a lattice problem is mapped into a self-consistent embedded impurity problem [3]. This mapping becomes exact in the limit of infinite spatial dimensions $d \rightarrow \infty$ due to the localization of the self-energy $\Sigma(\mathbf{k}, \omega) \rightarrow \Sigma(\omega)$ [4]. For finite dimensions DMFT is no longer exact, yet can be regarded as a useful approximation in which a purely local self-energy is assumed, hence the name dynamical mean field approximation (DMFA).

Applying the DMFA to study the properties of continuous Fermi gas, we first construct a lattice version of

the problem [5] and then seek the continuum limit which for finite gas densities corresponds to vanishing lattice filling.

The lattice formulation – The many-body Hamiltonian describing a dilute low energy Fermi gas is,

$$H = -\frac{\hbar^2}{2m} \sum_{\sigma} \int d\mathbf{x} \psi_{\sigma}^{\dagger}(\mathbf{x}) \nabla^2 \psi_{\sigma}(\mathbf{x}) + \frac{1}{2} V_0 \sum_{\sigma} \int d\mathbf{x} \psi_{\sigma}^{\dagger}(\mathbf{x}) \psi_{-\sigma}^{\dagger}(\mathbf{x}) \psi_{-\sigma}(\mathbf{x}) \psi_{\sigma}(\mathbf{x}), \quad (1)$$

where $\psi_{\sigma}(\mathbf{x})$ are the fermionic field operators. To construct a lattice version of this continuum Hamiltonian we represent the configuration space as an L^3 cubic lattice, where L is the number of sites in each spatial direction. The time direction is kept continuous. Next, we replace the position and momentum variables by the grid indices $\mathbf{x} \rightarrow \mathbf{n}$, $\mathbf{p} \rightarrow \frac{2\pi}{L} \mathbf{k}$, where \mathbf{n}, \mathbf{k} are integer vectors. The grid position and momentum are given by $a\mathbf{n}$ and \mathbf{p}/a , where a is the lattice spacing. The fermionic fields $\psi_{\sigma}(\mathbf{x}) \rightarrow (a)^{-3/2} \psi_{\mathbf{n}\sigma}$ are discretized to obey the anti-commutation relations $\{\psi_{\mathbf{n}\sigma}, \psi_{\mathbf{n}'\sigma}^{\dagger}\} = \delta_{\sigma\sigma'} \delta_{\mathbf{n}\mathbf{n}'}$. The corresponding lattice theory is the Hubbard Hamiltonian

$$H = -t \sum_{\sigma \mathbf{n} \mathbf{n}'} D_{\mathbf{n}\mathbf{n}'} \psi_{\mathbf{n}\sigma}^{\dagger} \psi_{\mathbf{n}'\sigma} + U \sum_{\mathbf{n}} \psi_{\mathbf{n}\uparrow}^{\dagger} \psi_{\mathbf{n}\uparrow} \psi_{\mathbf{n}\downarrow}^{\dagger} \psi_{\mathbf{n}\downarrow}, \quad (2)$$

where $t = \frac{\hbar^2}{2ma^2}$, and $U = V_0/a^3$. D is the hopping operator, $(D\psi_{\sigma})_{\mathbf{n}} = \sum_i (\psi_{\mathbf{n}+e_i, \sigma} - 2\psi_{\mathbf{n}, \sigma} + \psi_{\mathbf{n}-e_i, \sigma})$, where, e_j is a unit vector in the direction j . The spectra of the free lattice Hamiltonian is given by

$$\epsilon_{\mathbf{p}} = \frac{\hbar^2}{ma^2} D_{\mathbf{p}} \quad ; \quad D_{\mathbf{p}} = 2 \sum_i \sin^2 \frac{p_i}{2}. \quad (3)$$

In the following we shall use natural units setting $\hbar = m = 1$. The strength of the two-body interaction can be related to the two-body scattering length a_s through summation of the ladder diagrams for two-fermions interacting at zero energy, zero temperature and zero chemical potential, $\mu \rightarrow 0^-$, [6, 7]

$$\frac{1}{4\pi a_s} = \frac{1}{V_0} + \frac{C}{2a} \quad (4)$$

*Electronic address: nir@phys.huji.ac.il

where

$$C = \int_{-\pi}^{\pi} \frac{d\mathbf{p}}{(2\pi)^3} \frac{1}{D_{\mathbf{p}}} \approx 0.50532. \quad (5)$$

At unitarity $V_{0c} = -2a/C$, so $U_c = -7.91576t$. In contrast to the original continuum Hamiltonian (1), the lattice theory (2) acquires an effective range due to the finite lattice spacing. The ratio between this effective range, $r_{eff} \approx 2a/\pi^2$ [8], and the average interparticle distance is approximately $\frac{1}{2\pi} \sqrt[3]{n}$, where n is the average lattice filling, i.e. the number of particles per site. For finite lattice filling $0.1 \geq n \geq 0.01$ the corresponding average interparticle distance is roughly 12 to 24 times the effective range.

DMFA - Integrating out the fermionic degrees of freedom on all lattice sites but one - the impurity site - the DMFT maps the many-body Hamiltonian (2) into a single site effective action determined self-consistently from a bath with which the impurity site hybridizes. The impurity site can be taken to be a single lattice node [3] or a cluster of nodes [9]. Large cluster size improves the accuracy of the DMFA. As the computation complexity of the DMFA grows substantially with cluster size it is of great interest to assess the quality of the simplest approximation within this framework, namely the single node impurity.

Using the Nambu formalism, for a system with a superconducting long-range order, the impurity site effective action takes the form [3]

$$S_{eff} = - \int_0^{\beta} d\tau \int_0^{\beta} d\tau' \Psi^{\dagger}(\tau) \hat{\mathcal{G}}_0^{-1}(\tau - \tau') \Psi(\tau') - U \int_0^{\beta} d\tau c_{\uparrow}^{\dagger}(\tau) c_{\uparrow}(\tau) c_{\downarrow}^{\dagger}(\tau) c_{\downarrow}(\tau), \quad (6)$$

where $\beta = 1/T$ is the inverse temperature, $\Psi^{\dagger} \equiv (c_{\uparrow}^{\dagger}, c_{\downarrow})$ are the Nambu spinors, and $\hat{\mathcal{G}}_0(\tau)$ is given by

$$\hat{\mathcal{G}}_0(\tau) = \begin{pmatrix} \mathcal{G}_0(\tau) & \mathcal{F}_0(\tau) \\ \mathcal{F}_0^*(\tau) & -\mathcal{G}_0(-\tau) \end{pmatrix}. \quad (7)$$

In the following we shall use the "hat" notation for the Nambu matrices. The corresponding impurity Green's function is given by

$$\hat{\mathcal{G}}(\tau) \equiv -\langle T \Psi_i(\tau) \Psi_i^{\dagger}(0) \rangle_{S_{eff}} = \begin{pmatrix} \mathcal{G}(\tau) & \mathcal{F}(\tau) \\ \mathcal{F}^*(\tau) & -\mathcal{G}(-\tau) \end{pmatrix}, \quad (8)$$

where $\mathcal{G}(\tau) = -\langle T c_{\sigma}(\tau) c_{\sigma}^{\dagger}(0) \rangle_{S_{eff}}$ and $\mathcal{F}(\tau) = -\langle T c_{\uparrow}(\tau) c_{\downarrow}(0) \rangle_{S_{eff}}$.

In the DMFA the interaction effects are taken into account through the self-energy matrix

$$\hat{\Sigma}(i\omega_n) = \begin{pmatrix} \Sigma(i\omega_n) & S(i\omega_n) \\ S(i\omega_n) & -\Sigma^*(i\omega_n) \end{pmatrix} \quad (9)$$

deduced from the Dyson equation

$$\hat{\Sigma}(i\omega_n) = \hat{\mathcal{G}}_0^{-1}(i\omega_n) - \hat{\mathcal{G}}^{-1}(i\omega_n), \quad (10)$$

where $\omega_n = (2n+1)\pi/\beta$ are the Matsubara frequencies. Here and in the following, we have assumed that the symmetry of the pairing is such that the off diagonal self energy obeys $S(i\omega_n) = S^*(-i\omega_n)$. The connection to the physical lattice is made through the self-consistency requirement that the impurity Green's function is equal to the local lattice Green's function $\hat{\mathcal{G}}(\tau) = \hat{G}(\tau)$, or $\mathcal{G}(\tau) = G(\tau)$, and $\mathcal{F}(\tau) = F(\tau)$, where

$$G = \sum_{\mathbf{k}} \frac{-i\omega_n + \mu - \epsilon_{\mathbf{k}} - \Sigma^*(i\omega_n)}{|i\omega_n + \mu - \epsilon_{\mathbf{k}} - \Sigma(i\omega_n)|^2 + S^2(i\omega_n)},$$

$$F = - \sum_{\mathbf{k}} \frac{S(i\omega_n)}{|i\omega_n + \mu - \epsilon_{\mathbf{k}} - \Sigma(i\omega_n)|^2 + S^2(i\omega_n)}. \quad (11)$$

Solving the Impurity Model - Caffarel and Krauth [10] proposed to approximate the effective impurity action through an Anderson model

$$\begin{aligned} \mathcal{H}_{And} &= \mathcal{H}_0 + \mathcal{H}_I \\ &= \sum_{l,\sigma} \tilde{\epsilon}_l a_{l\sigma}^{\dagger} a_{l\sigma} + \sum_{l,\sigma} \tilde{V}_l (a_{l\sigma}^{\dagger} c_{\sigma} + c_{\sigma}^{\dagger} a_{l\sigma}) \\ &\quad + \sum_{l,\sigma} \tilde{D}_l (a_{l\sigma}^{\dagger} c_{-\sigma}^{\dagger} + c_{-\sigma} a_{l\sigma}) + U n_{\uparrow} n_{\downarrow}, \end{aligned} \quad (12)$$

where the interaction of the fermionic field c_{σ} with the auxiliary bath fermions $a_{l\sigma}$ generate both the normal and abnormal components of the "free" impurity Green's function $\mathcal{G}_0, \mathcal{F}_0$. This goal is achieved by choosing the parameters of the Anderson model $\tilde{\epsilon}_l, \tilde{V}_l, \tilde{D}_l$ to minimize the difference between the $\hat{\mathcal{G}}_0$ and $\hat{\mathcal{G}}_0^{And}$ over a finite range of frequencies $|\omega_n| \leq \omega_N$. The "free" Anderson's Green's function $\hat{\mathcal{G}}_0^{And}$ is calculated by numerical inversion of \mathcal{H}_0 . When the number n_s of fermionic fields, a_l and c , is smaller than 6 standard diagonalization methods can be used to solve \mathcal{H}_{And} . For $T = 0$ the Lanczos method makes a calculation with as many as $n_s = 10$ fermionic fields feasible [3].

Extracting the Physics - Solving the DMFA equations yields the local approximation for the self-energy $\hat{\Sigma}(\mathbf{k}, i\omega_n) \approx \hat{\Sigma}(i\omega_n)$, and correspondingly

$$G(\mathbf{k}, i\omega_n) = \frac{-i\omega_n + \mu - \epsilon_{\mathbf{k}} - \Sigma^*(i\omega_n)}{|i\omega_n + \mu - \epsilon_{\mathbf{k}} - \Sigma(i\omega_n)|^2 + S^2(i\omega_n)}, \quad (13)$$

and

$$F(\mathbf{k}, i\omega_n) = - \frac{S(i\omega_n)}{|i\omega_n + \mu - \epsilon_{\mathbf{k}} - \Sigma(i\omega_n)|^2 + S^2(i\omega_n)}. \quad (14)$$

Once G and F are known, thermodynamic quantities such as the number of particles per site, the energy, and the superconducting gap can be calculated through the Matsubara sums,

$$n = \frac{1}{\beta} \sum_{\sigma\mathbf{k}} \sum_{n=-\infty}^{\infty} e^{i0^+} G(\mathbf{k}, i\omega_n) \quad (15)$$

$$\Delta_0 = \frac{U}{\beta} \sum_{\mathbf{k}} \sum_{n=-\infty}^{\infty} e^{i0^+} F(\mathbf{k}, i\omega_n) \quad (16)$$

and

$$E = \frac{1}{2} \frac{1}{\beta} \sum_{\sigma \mathbf{k}} \sum_{n=-\infty}^{\infty} e^{i0^+} (i\omega_n + \epsilon_{\mathbf{k}} + \mu) G(\mathbf{k}, i\omega_n). \quad (17)$$

The number of particles n and the gap Δ_0 can also be calculated directly from the Anderson's Hamiltonian (12). If $\hat{G} = \hat{G}$ these results would coincide. However, at best $\hat{G} \approx \hat{G}$, so this is not always the case. Since the Matsubara sum contains explicit dependence on the lattice density of state it provides a more reliable estimate for n and Δ_0 . We shall use the relative difference $\delta_n = (n_M - n_{And})/n_M$ between the Matsubara density n_M and the Anderson's model density n_{And} as a measure for the quality of the impurity solution. For very accurate solution of the impurity model we expect that $\delta_n \ll 1$. When δ_n deviates substantially from zero it is an indication that the number of auxiliary fields we have used in the solution of (6) is not sufficient.

Direct evaluation of the Matsubara sums is impractical. Having calculated $\Sigma(i\omega_n), S(i\omega_n)$ over a finite range of frequencies we evaluate the thermodynamic observables in the following manner. We set $\Sigma_{\infty} = \text{Re}(\Sigma(i\omega_N))$, and $S_{\infty} = S(i\omega_N)$, assuming that at ω_N , the largest frequency we explicitly consider, the self-energy has already acquired its asymptotic value. Using these quantities we construct the Green's function components G_{∞}, F_{∞} by the appropriate substitutions of $\Sigma_{\infty}, S_{\infty}$ in Eqs. (13), (14). The Matsubara sums with G_{∞}, F_{∞} are evaluated analytically to obtain n_{∞}, E_{∞} etc. Then for the frequencies in the range $|\omega_n| \leq \omega_N$ we calculate the difference between G and G_{∞} to obtain

$$n = n_{\infty} + \frac{1}{\beta} \sum_{\sigma \mathbf{k}} \sum_{n=-N}^N (G(\mathbf{k}, i\omega_n) - G_{\infty}(\mathbf{k}, i\omega_n)), \quad (18)$$

and equivalently for any other thermodynamic observable of interest.

Results – The attractive Hubbard model and the BCS-BEC cross were originally studied within the DMFT by Keller *et. al* [11] who have established the phase diagram of the system at quarter filling $n = 1/2$ using a half-ellipse density of states. Later on this work was followed by [12, 13, 14] who have studied different aspects of the transition in the limit $d \rightarrow \infty$. In [5] we have studied the continuum limit of the metastable Fermi liquid phase in $d = 3$. Here we extend this study to the ground state superconducting phase. The properties of a Fermi gas with attractive interaction were studied by different groups using different techniques [15, 16, 17, 18, 19]. At unitarity, it is customary to present the $T = 0$ ground state energy per particle in the form $E/N = \xi E_{FG}$ where $E_{FG} = 0.6E_F$ and E_F is the Fermi energy. The value $\xi = 0.44 \pm 0.01$ was calculated by [15, 16, 17], using the fixed-node diffusion Monte-Carlo (DMC) method. In Fig. 1 we present the energy per particle $T = 0$ DMFA results as a function of the interaction strength in comparison with the DMC results. It can be seen that the

DMFA results are in agreement with the DMC calculations.

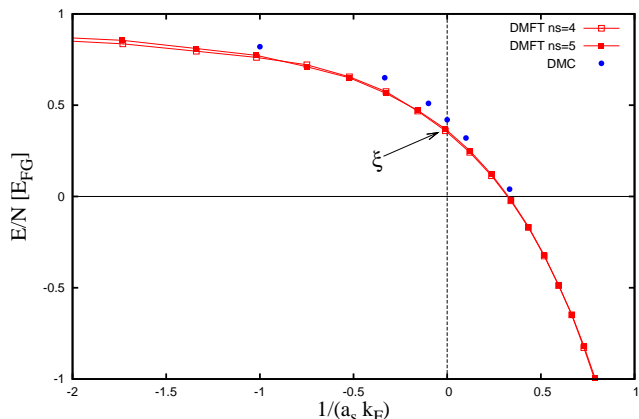


FIG. 1: (Color online) The $T = 0$ energy per particle as a function of the dimensionless parameter $1/(a_s k_F)$. DMFA at lattice filling of $n = 0.1$ with $n_s = 4, 5$ are denoted by filled and empty squares. The circles are the DMC of [17].

Since the continuum corresponds to the limit of vanishing lattice filling we explore in Fig. 2 the dependence at unitarity of E/N and the gap function Δ_0 on n . As the lattice filling approach zero the accuracy of our calculation deteriorates since with $n_s \leq 6$ the bath fermions are unable to reproduce the fine details of \hat{G}_0 needed for such calculation. To demonstrate this point we attached to each data point an error bar, $\delta_n(E/N)$ to the energy points and $\delta_n \Delta_0$ to the gap points, where δ_n is the relative density error discussed above. From the figure we can see that as expected the error decrease with the number of auxiliary fields. It can also be seen that the error grows substantially at the lower most densities. Extrapolating the $n_s = 6$ calculation to the continuum limit we obtain $\xi \approx 0.44$ and $\Delta_0 \approx 0.64E_F$. These values are in close agreement to the Quantum Monte-Carlo (QMC) calculations of [16, 17, 19].

Turning now to study the behavior of the system at finite temperature we present in Fig. 3 the energy per particle, the chemical potential and the superconducting gap at unitarity as a function of temperature for lattice filling $n = 0.1$. From the figure one can clearly identify the superconducting phase transition associated with the vanishing of the superconducting gap and the discontinuity in the derivatives of μ and E . Similar qualitative behavior was already identified by Bulgac *et. al* [18]. The critical temperature $T_c \approx 0.16E_F$ is somewhat smaller than their result $T_c = 0.23E_F$ but agrees with the value $T_c = 0.15E_F$ of Burovski *et. al* [20]. In the superconducting region, the gap function behaves approximately as $\Delta_0(T) = \Delta_0(0)(1 - (T/T_c)^\kappa)$ and the energy as $E(T) = NE_{FG}(\xi + \zeta(T/T_c)^\lambda)$. Comparing the DMFA results with these formulas we have found that $\kappa \approx 7$, and $\lambda \approx 5$. These values are substantially higher than the QMC values $\kappa = 1.5, \lambda = 2.5$ found in [18]. An exper-

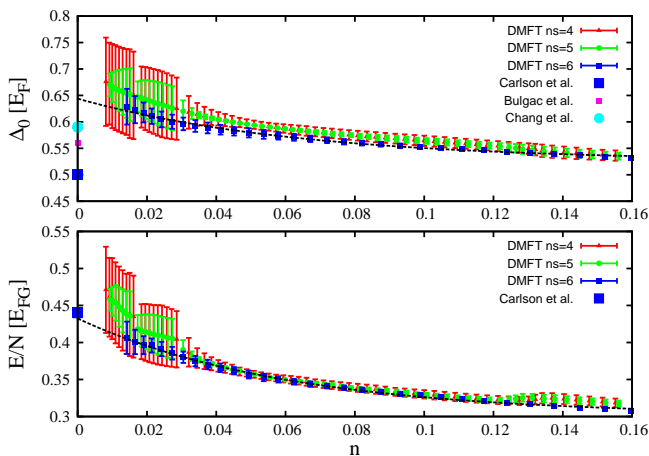


FIG. 2: (Color online) The $T = 0$ energy per particle and superconducting gap as a function of the lattice filling n . The DMFA calculation with $n_s = 4$ are shown with triangles, $n_s = 5$ with circles, and $n_s = 6$ with squares. Also shown are the QMC results of [15, 17, 19].

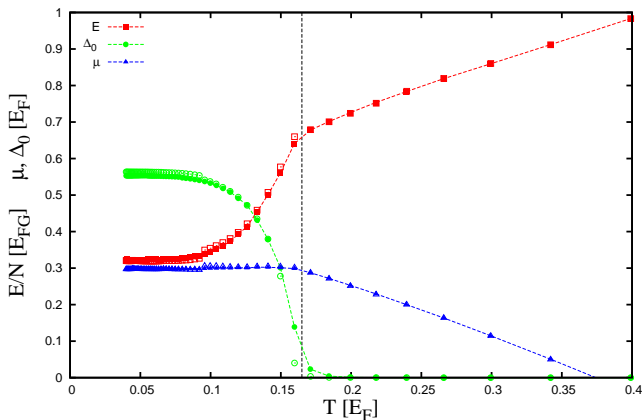


FIG. 3: (Color online) The temperature dependence of E , μ , Δ_0 at unitarity, for lattice filling $n = 0.1$. The energy per particle E/N is shown with squares, the chemical potential μ is shown with triangles, and the gap function Δ_0 is shown with circles. Calculations with $n_s = 6$ are shown with filled shapes, calculations with $n_s = 5$ with empty ones.

imental indication for a large λ can be found in [21] were the value $\lambda = 3.73$ was reported. for a unitary Fermi gas in a trap. It is interesting to note that in contrast with the observation of Toschi *et. al* [22] our calculations seems to indicate a coincidence between the disappearance of the gap and the discontinuity of the heat capacity. Thus Δ_0 provides no indications for a phase transition associated with the closure of a pseudo gap above T_c . On the other hand, in our calculations the gap function Δ_0 doesn't vanish at $T = T_c$ but, like the other thermodynamic variables, change its behavior and drops to zero exponentially.

Conclusions – In this work we have applied the DMFA to study the properties of a unitary Fermi gas. We have found that the predictions of this theory agree remarkably well with the results of full QMC simulations. The DMFA energy per particle actually coincide with the results of the fixed node Monte-Carlo simulations, whereas the gap function is somewhat higher than previous estimates. At finite temperature the DMFA results agree qualitatively with those of [18] although the thermodynamic functions exhibit a stronger temperature dependence. These results indicate that the self-energy of a dilute Fermi gas has only a weak momentum dependence, since by construction the DMFA equations yields the local approximation for the self-energy $\hat{\Sigma}(\mathbf{k}, i\omega_n) \approx \hat{\Sigma}(i\omega_n)$. The momentum dependence of $\hat{\Sigma}(i\omega_n)$ can be investigated by extending the impurity site from a single node into a cluster of nodes. The DMFA results can be further refined using a QMC approach at finite temperature or the Lanczos diagonalization method at $T = 0$.

I wish to thank A. V. Andreev, G. F. Bertsch, A. Bulgac, S. Y. Chang and D. Gazit for useful discussions and help during the preparation of this work. This work was supported by the Department of Energy Grant No. DE-FG02-00ER41132.

[1] P. Courteille, R. S. Freeland, D. J. Heinzen, F. A. van Abeelen, B. J. Verhaar, Phys. Rev. Lett. **81**, 69 (1998).
 [2] A. Georges, G. Kotliar, Phys. Rev. B **45**, 6479 (1992).
 [3] A. Georges, G. Kotliar, W. Krauth, M. Rozenberg, Rev. Mod. Phys. **68**, 13 (1996).
 [4] W. Metzner, D. Vollhardt, Phys. Rev. Lett. **62**, 324 (1989).
 [5] N. Barnea, Phys. Rev. B **77**, 020501(R) (2008).
 [6] T. Papenbrock and G. F. Bertsch, Phys. Rev. C **59**, 2052 (1999).
 [7] J. W. Chen, D. B. Kaplan, Phys. Rev. Lett. **92**, 257002 (2004).

[8] H. Esbensen, G. F. Bertsch, K. Hencken, Phys. Rev. C **56**, 3054 (1997).
 [9] T. Maier, M. Jarrell, T. Puschke, and M. H. Hettler, Rev. Mod. Phys. **77**, 1027 (2005).
 [10] M. Caffarel, W. Krauth, Phys. Rev. Lett. **72**, 1545 (1994).
 [11] M. Keller, W. Metzner, U. Schollwöck, Phys. Rev. Lett. **86**, 4612 (2001).
 [12] M. Capone, C. Castellani, M. Grilli, Phys. Rev. Lett. **88**, 126403 (2002).
 [13] A. Toschi, M. Capone, and C. Castellani, Phys. Rev. B **72**, 235118 (2005).

- [14] A. Garg, H. R. Krishnamurthy, and M. Randeria, Phys. Rev. B **72**, 024517 (2005).
- [15] S. Y. Chang, V. R. Pandharipande, J. Carlson, K. E. Schmidt, Phys. Rev. A **70**, 043602 (2004).
- [16] G. E. Astrakharchik, J. Boronat, J. Casulleras, S. Giorgini, Phys. Rev. Lett. **93**, 200404 (2004).
- [17] J. Carlson, S.-Y. Chang, V. R. Pandharipande, K. E. Schmidt, Phys. Rev. Lett. **91**, 050401 (2003).
- [18] A. Bulgac, J. E. Drut, and P. Magierski, Phys. Rev. Lett. **96**, 090404 (2006).
- [19] A. Bulgac, J. E. Drut, P. Magierski, and G. Wlazlowski, arXiv: 0801.1504v1 [cond-mat.stat-mech].
- [20] E. Burovski, N. Prokof'ev, B. Svistunov, and M. Troyer Phys. Rev. Lett. **96**, 160402 (2006).
- [21] J. Kinast *et. al*, Science **307**, 1296 (2005).
- [22] A. Toschi, P. Barone, M. Capone, and C. Castellani, New J. Phys. **7**, 7 (2005).